Method for pressure and flow calculations of a 5GDHC grid with bidirectional energy flow and non-directional medium flow

Lindhe, Jonas

2022

LUND UNIVERSITY

PO Box 117
221 00 Lund
+46 46-222 00 00

Method for pressure and flow calculations of a 5GDHC grid with bidirectional energy flow and non-directional medium flow

Jonas Lindhe

Avdelningen för installationsteknik
Institutionen för bygg- och
miljöteknologi Lunds tekniska högskola
Lunds universitet, 2022
Rapport TVIT--22/7129

Lunds Universitet

Lunds Universitet, med nio fakulteter samt ett antal forskningscentra och specialhögskolor, är Skandinaviens största enhet för forskning och högre utbildning. Huvuddelen av universitetet ligger i Lund, som har 100 400 invånare. En del forsknings- och utbildningsinstitutioner är dock belägna i Malmö, Helsingborg och Ljungbyhed. Lunds Universitet grundades 1666 och har idag totalt 6 000 anställda och 41 000 studerande som deltar i ett 90-tal utbildningsprogram och ca 1000 fristående kurser erbjudna av 88 institutioner.

Avdelningen för installationsteknik

Avdelningen för Installationsteknik tillhör institutionen för Bygg- och miljöteknologi på Lunds Tekniska Högskola, som utgör den tekniska fakulteten vid Lunds Universitet. Installationsteknik omfattar installationernas funktion vid påverkan av människor, verksamhet, byggnad och klimat. Forskningen har en systemanalytisk och metodutvecklande inriktning med syfte att utforma energieffektiva och funktionssäkra installationssystem och byggnader som ger bra inneklimat.
Nuvarande forskning innefattar bl a utveckling av metoder för utveckling av beräkningsmetoder för godtyckliga flödessystem, konvertering av direktelvärmda hus till alternativa värmesystem, vädring och ventilation i skolor, system för brandsäkerhet, alternativa sätt att förhindra rökspridning vid brand, installationernas belastning på yttre miljön, att betrakta byggnad och installationer som ett byggnadstekniskt system, analysera och beräkna inneklimatet i olika typer av byggnader, effekter av brukarnas beteende för energianvändning, reglering av golvvärmesystem, bestämning av luftflöden i byggnader med hjälp av spårgasmetod. Vi utvecklar även användbara projekteringsverktyg för energi och inomhusklimat, system för individuell energimätning i flerbostadshus samt olika analysverktyg för optimering av ventilationsanläggningar hos industrin.

Method for pressure and flow calculations of a 5GDHC grid with bidirectional energy flow and non-directional medium flow

Jonas Lindhe

ISRN LUTVDG/TVIT-22/7129-SE(36)

Installationsteknik
Institutionen för bygg- och miljöteknologi
Lunds tekniska högskola
Lunds universitet
Box 118
221 00 LUND

Acknowledgement:

For the work in developing the formulas, I want to thank professor emeritus Johan Claesson at the Department of Building and Environmental Technology for the cooperation, help and support.

Contents

Introduction:

The development of our society is dependent upon access to energy. Energy for heating and cooling accounts for 50% of final energy consumption within the European union. Today, 75% of the energy use within the energy sector is based on fossil fuels and only 18% comes from renewable energy sources [1]. The use of fossil fuels negatively affects our environment. Therefore, the use of fossil-based energy must be reduced by more efficient use of energy and replacement by renewable energy generation.

There is no universal solution to this problem. To achieve the energy transition, a mixture of measures based on renewable and recycled energy combined with energy efficiency will be required.

The European commission published a strategy in 2016 that provides a framework for integrating efficient use of energy for heating and cooling [1]. One of the identified measures is the reuse of excess energy flows within the community. This requires an approach in the design/construction of our energy systems which enables the recovering and sharing of energy flows between buildings, reducing the primary energy demand. One challenge in the ability of recovering energy flows is the temperature quality. For example, there can be lots of excess energy flowing from a source that cannot be recovered due to its low temperature level. This is a common issue in urban areas due to the variety of energy flows that appears, such as low temperature sewage water.

In parts of Europe, it is common to build centralized heating and cooling facilities and distribute the energy through a grid. These are commonly referred to as district energy systems. The first district heating solution was introduced around 1880 and used steam as the energy carrier, distributed in steel pipes to the customer[2][3][4]. In the following generations of district heating, water has replaced steam and the focus has been on lowering the temperature levels and material costs of the grid.

Fifth generation district heating and cooling (5GDHC) is under development, partly in parallel to the development of the fourth generation. 5GDHC works with temperatures near ground temperatures (6-40°C), which is lower than previous generations. This makes it possible to integrate energy flows with different temperature qualities and to recover low exergy heat sources. The temperature levels in the 5GDHC grid are free and only limited by installed materials characteristics or operational strategies. Materials such as uninsulated plastic pipes can replace the more traditional insulated steel pipes in 5GDHC grids.

The previous generations are based on larger centralised energy production units with a high temperature distribution grid (60-120°C) covering whole or large parts of cities. Parallel to the district heating grid, there can be a district cooling grid with a central cooling facility based on cooling machines and free cooling sources.

The 5GDHC is a more complex solution. It is based upon the shared energy principle which means an energy system that is designed for recovering and using excess energy flows before putting in external energy. In a 5GDHC solution the primary focus is on balancing energy imbalances within and between buildings before using external energy. The working principle is that an individual building extracts heat or cold energy from the grid and when doing so the grid also receives excess energies of cold or heat. Recovered energies are then shared to other buildings or saved in a thermal energy storage. In the ideal 5GDHC solution, there is no need for an external energy source and only local heat pumps for combined cooling and heating are installed in each building.

The grid has no supply and return pipe, instead there is a cold and warm pipe which makes it possible to distribute both cooling and heating within the same pipes. The grid is designed to handle a bidirectional energy flow and non-directional medium flow.

There are several challenges with the adoption of the new 5GDHC energy solution. This solution is more complex than previous district energy solutions and requires more coordination between the connected facilities. For the grid to run efficiently, each building's demands and assets need to be coordinated toward other buildings and joint balancing units, such as seasonal energy storage and accumulators. Therefore, a more advanced central control for operating and optimisation of the solution is needed.

The overall control system tries to fulfil the chosen operation strategy as efficiently as possible and takes into account different parameters, such as availability of thermal inertia, weather data and excess energy flows. The central control system also handles business transactions within the grid. These are some examples of parameters which need to be integrated in the development of overall control systems.

There are also challenges in adapting and development of heat pump equipment. Local heat pumps (in buildings connected to the grid) need to be able to work within a broader temperature width (6 to 40˚C) than normal on the evaporator side. Central heat pumps (used to balance energy imbalances in the grid) require adaptions on the condenser side to meet the lowest grid temperatures (6 to 16˚C) on the condenser side.

Accurate tools for design and simulation of 5GDHC grids are not fully developed. Unlike previous tools for district heating, these must be able to handle both bidirectional energy flows and non-directional medium flows. Furthermore, these tools must allow for the calculation of mass flows, pressure levels and heat losses or gains in the grid, in order to design efficient solutions and show the consequences of different operation strategies. The calculation of heat-losses or gains is important for the design and development of 5GDHC grids. Sometimes the grid is designed and built with uninsulated distribution pipes. There is a need for a tool to evaluate the heat losses due to different design choices.

The aim of this study is to develop a continuous calculation method that calculates pressure and mass flows in a meshed, non-directional medium flow and bidirectional energy flow in a two pipe 5GDHC grid solution. Such a method can be used for modelling, design and dimensioning purposes. A method that easily handles load changes in the grid, facilitates the calculation of heat losses and operational costs of the grid. Such method also enlightens the consequences of changes in the grid design or changed operational strategy and can be used for monitoring purposes. Such calculation method is one piece of the puzzle for developing a dynamic simulation model for 5GDHC systems.

This article reports the calculation method, its derivation and application. The article is the first step of developing a new calculation method. There are needs for further verification and tests.

Existing pressure calculation methods for 5GDHC solutions

There is lack of methods that calculates pressure levels in a bidirectional meshed grid without using a design/reference point as a base. It requires time-consuming work before various changes, which impact the reference point, are possible to perform. During an initial design phase, this might limit the investigation of possible designs or expanding strategies.

Previous research on pressure simulations of a 5GDHC grid used a modelica based library. This library calculates the mass flow based on the original design pressure at a certain flow and from that calculates the new reference conditions[5][6][7][8][9]:

$$\dot{m} = sign(\Delta P)k\sqrt{\Delta P} \text{ ,} \tag{1.1.1}$$

where k refers to a system constant reflecting the characteristics of the system. The system constant is used for adjusting deviations between the calculation and known measurements [10].

The formula is based upon the assumption of ideal affinity law that defines the square relationship between pressure and flow, which normally dominates the pressure losses.

By knowing of the massflow and pressure in the design/reference point and the massflow in the point of interest , it is possible to calculate that new pressure level. If the system is changed, e.g. other pipe dimensions, additional pipes, more fittings or another fluid, then a new design/reference point needs to be calculated and also the k is then unknown.

A technical design framework for cold heating and cooling networks has also been published within the KoWaNet project [11] in Netherlands. The pressure calculation is based on the traditional moody diagram and Colebrook-white equation. This is used for retrieving the specifications for pumps or calculating the design point that is used in previously mentioned modelica simulation.

There are also advanced dynamic simulation programs used for simulating traditional district heating grids, such as Netsims. Referring to the manual [12] the pressure calculation in Netsims is performed by using:

$$\Delta p = (K_1 + K_2 * D) * \varphi * \left(\frac{2 * u^2 * L * c_f}{D} + g * (z_d - z_u) \right), \tag{1.1.2}$$

where K1 and K2 are calibration constants used for adjusting discrepancies between measured and calculated data, D is the pipe diameter (m), and u is velocity (m/s). The friction factor, c_f is calculated by using Colebrook – White's formula. The formula also includes any pressure difference that appears due to static pressure, (ρ∗g*Δz) were z is the level over a reference point (m). Even if the static pressure does not influence the friction based pressure losses, it is good to know to assess the risk for cavitation in pumps and verify that pressure limits is not exceeded. The formula **Fel! Hittar inte referenskälla.** 1.1.2 cannot handle bidirectional flows.

In the Modellica standard library [13] online there are a similar approach as presented in this article for calculating non directional medium flow in a grid. That calculation method needs to define a static pressure so that the pressure never becomes negative.

Development of a new continuous method for flow and pressure calculation of a 5GDHC two pipe solution

Flow pressure calculation for any pipe segment

Figure 3.1 shows a pipe with flowing water. The length of the considered pipe is L_p (m). L_{eq} (m) is the equivalent pipe length compensating for local losses, e.g. bends and valves, and the pipe inner diameter is D (m). L (m) is the total length of the pipe L_p and L_{eq}. The calculation of L_{eq} is accounted for in a separate section. The pressure drop over the pipe and fittings is Δp (N/m^2). The bulk water velocity is u (m/s) and the corresponding mass flow is $\dot{m}$ (kg/s). The water density is ρ (kg/m^3) and the viscosity μ (Ns/m^2 or kg/(m·s). The water flow may be positive, zero or negative. The velocity and mass flow become negative for negative *Δp.*

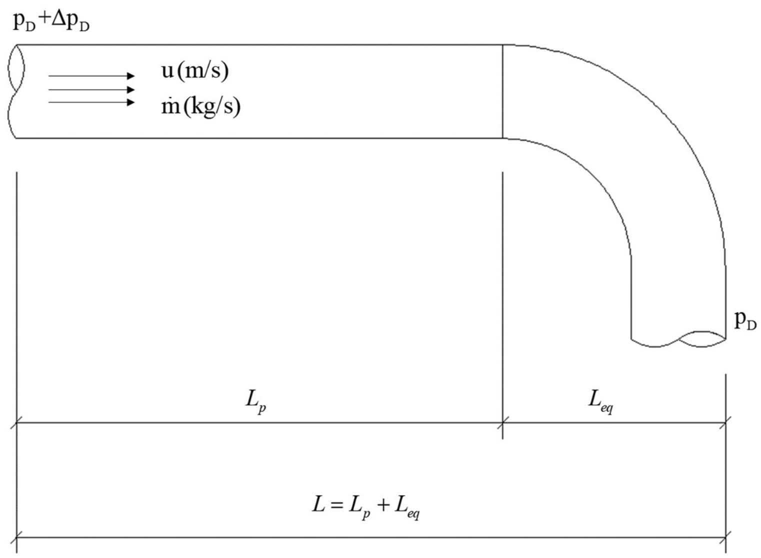

Figure 3.1. Notations for the considered pipe segment.

The mass flow is proportional to the bulk velocity. In the formulae below, it is convenient to allow Reynolds' number to be negative for negative u:

$$\dot{m} = \rho \cdot \pi (D/2)^2 \cdot u; \qquad \mathrm{Re} = \frac{\rho D u}{\mu}, \qquad \mathrm{Re}_{\mathrm{tr}} = 2000. \tag{2.1.1}$$

The transition from laminar to turbulent flow occurs around $|\,\mathrm{Re}\,| = \mathrm{Re}_{\mathrm{tr}} = 2000.$

Pressure flow formula for laminar and turbulent flow

Pressure-flow formulas for laminar and turbulent flow may be found in many books on mass transfer, for example Kay and Nedderman, An introduction to Fluid Mechanics and Heat Transfer [14]. The standard formula for pressure drops in pipes is the Darcy – Weisbach equation were the c_f is a friction coefficient. In this method, the Darcys – Weisbach friction coefficient is used. The c_f for *laminar* flow in a circular, smooth pipe is valid when the magnitude of the Reynolds number is smaller than a transition value of 2 000; otherwise, it is a turbulent flow.

The friction coefficient c_f for laminar flow is calculated as $c_f = \dfrac{64}{\mathrm{Re}}$

The total length L is calculated as $L = L_p + \Sigma L_{eq}$

$$\left|\mathrm{Re}\right| < \mathrm{Re}_{\mathrm{tr}}: \quad \Delta p = c_f \cdot \frac{L}{D} \cdot \frac{\rho u^2}{2} = \frac{32}{\mathrm{Re}} \cdot \frac{L}{D} \cdot \rho u^2 = \frac{32\,\mu\,L\,u}{D^2} = \frac{32\,\mu\,L}{D^2} \cdot \frac{\mu\,\mathrm{Re}}{\rho\,D} = \frac{32\,\mu^2}{\rho} \cdot \frac{L}{D^3} \cdot \mathrm{Re} \tag{2.1.2}$$

Calculating c_f for turbulent flow is performed by the use of Colebrook-White’s formula which requires a trial and error approach. There are however approximate formulae for calculating c_f directly, such as Blasius formula or Swamee – Jain. Blasius formula is used for smooth pipes, for example some plastic pipes, as it does not take pipe roughness in consideration; where as Swamee-Jain takes pipe roughness into account.

The Swamee-Jain formula was used in this method for calculating c_f, so no consideration needs to be taken whether the pipes are smooth or not. The absolute roughness is e (mm) and e_m is the absolute roughness in meters (m).

$$e_m = \frac{e}{1000} \quad (\mathrm{m}).$$

The formula for pressure calculation of turbulent flow in a circular pipe using Swamee-Jain formula is:

$$|Re| > Re_{tr}: \quad \Delta P = c_f \cdot \frac{L}{D} \cdot \frac{\rho u|u|}{2}, \; c_f \cdot \frac{1}{(4\log(y))^2}, \; y = \frac{e_m}{3{,}7D} + \frac{5{,}74}{(|Re|)^{0{,}9}}. \tag{2.1.3}$$

It should be noted that the normally occurring factor u^2 is replaced by $u\cdot|u|$ to order to include the case of negative u-values (opposite flow direction). A “normalized” Reynolds number x is introduced to distinguish the turbulent and laminar areas.

$$x = \frac{\mathrm{Re}}{\mathrm{Re}_{\mathrm{tr}}} = \frac{\rho\,D\,u}{\mu\,\mathrm{Re}_{\mathrm{tr}}}. \tag{2.1.4}$$

The above formulas (2.1.3) and (2.1.4) may be rewritten:

$$\Delta p = \frac{1}{4} \cdot \frac{1}{(\log(y))^2} \cdot \frac{L}{D} \cdot \frac{\rho \cdot u \cdot \left|u\right|}{2} = \frac{\rho}{8} \cdot \frac{L}{D} \cdot \left(\frac{\mu \cdot \mathrm{Re}_{tr}}{\rho \cdot D}\right)^2 \cdot \frac{x\left|x\right|}{(\log(y))^2}. \tag{2.1.5}$$

The constants k_0 (N) and k_1 (-) are now introduced:

$$k_0 = \frac{32\,\mu^2}{\rho} \cdot \mathrm{Re}_{\mathrm{tr}}, \qquad k_1 = \frac{\mathrm{Re}_{\mathrm{tr}}}{256}. \tag{2.1.6}$$

The formula 2.1.5 can know be rewritten:

$$\Delta p = \frac{\rho}{8} \cdot \frac{L}{D} \cdot \frac{\mu \cdot \mathrm{Re}_{tr}}{\rho \cdot D} \cdot \frac{x\,|x|}{(\log(y))^2} \cdot \frac{k_0}{32 \cdot \mu \cdot D} = \frac{L}{D^3} \cdot k_0 \cdot \frac{k_1 \cdot x\,|x|}{(\log(y))^2} \tag{2.1.7}$$

The flow is laminar for -1 < x < 1, and it is turbulent for x > 1 and x < -1.

The following combined formula are obtained from (2.1.2), (2.1.6) and (2.1.7):

$$\Delta p = k_0 \cdot \frac{L}{D^3} \cdot f_{p0}(x, e'), \quad x = \frac{\mathrm{Re}}{\mathrm{Re}_{\mathrm{tr}}} = \frac{\rho\, D\, u}{\mu\, \mathrm{Re}_{\mathrm{tr}}}, \qquad e' = \frac{e_m}{D}. \tag{2.1.8}$$

$$f_{p0}(x, e') = \begin{cases} x & |x| < 1 \\ \dfrac{k_1\, x\, |x|}{(\log(y))^2} & |x| > 1 \end{cases}, \quad y = \frac{e'}{3,7} + \frac{5,74}{(|\mathrm{Re}|)^{0,9}}. \tag{2.1.9}$$

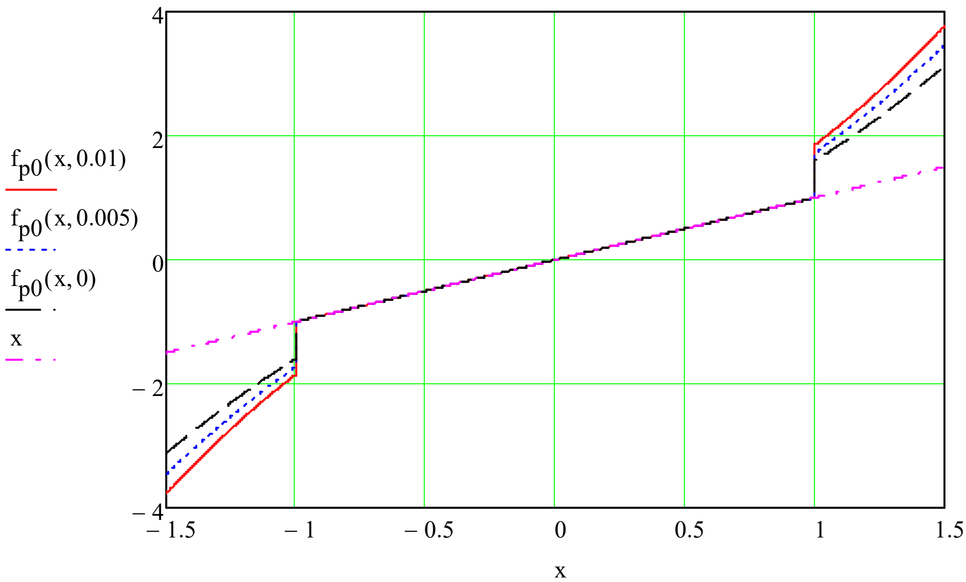

Figure 3.2. Flow function $f_{p0}(x,e')$

The dimensionless flow function $f_{p0}(x,e')$ is an odd function in x that increases monotonously with x, this is shown in Fig. 3.2, (k1=7,8125). The figure shows the function in the laminar and turbulent areas. The red dotted curve illustrates the laminar area when -1 < x < 1, the curves follows x. When x > 1 and x < -1, the curves illustrates the turbulent area which is dependent upon the influence of pipe roughness, e, and therefor the curves differs from each other. The flow function is discontinuous at x = 1 and x = -1.

The flow formula (2.1.8) gives the pressure drop as a function of x or *u*. An alternative is to use x as a function of the mass flow $\dot{m}$:

$$\dot{m} = \frac{\pi\,\rho\,D^2\cdot u}{4} = \frac{\pi\,\mu\,D\cdot\mathrm{Re}}{4}, \qquad x = \frac{\mathrm{Re}}{\mathrm{Re}_{\mathrm{tr}}} = \frac{4\,\dot{m}}{\pi\,\mu\,D\cdot\mathrm{Re}_{\mathrm{tr}}} = \frac{\dot{m}}{k_2\cdot D}; \qquad k_2 = \frac{\pi\,\mu\,\mathrm{Re}_{\mathrm{tr}}}{4}. \tag{2.1.10}$$

In the equation above, k_2 is a constant that has the same unit as the viscosity, (kg/(m·s)).

Modified, continuous flow-pressure formula

The above flow function is discontinuous at the transition between laminar and turbulent flows. This means that the flow is indeterminant at x = 1 and x = -1. The flow pattern may in certain cases be indeterminant for the networks analysed below.

The remedy is to make the flow function continuous, while essentially keeping the relations in laminar and turbulent regions. The laminar expression x is used for -1 < x < 1, and the turbulent expression is used for x > 1+Δx and x < -1-Δx. Here, Δx is small compared to 1. A linear interpolation is used for the transition regions. The following expressions for the modified flow function are obtained:

$$f_p(x,e') = \begin{cases} f_{po}(x,e') & -1 < x < 1, \quad x \geq 1+\Delta x, \quad x \leq -1-\Delta x \\ 1+\Delta f\cdot(x-1) & 1 \leq x \leq 1+\Delta x \\ -1+\Delta f\cdot(x+1) & -1-\Delta x \leq x \leq -1 \end{cases}$$

$$\Delta f = \frac{f_{p0}(1+\Delta x, e') - 1}{\Delta x} \tag{2.1.11}$$

The two linear parts define the dimensionless slope Δf in the transition regions:

$$x = 1:\;\; f_p(1,e') \to 1 + \Delta f(1-1) = 1, \;\; x = -1:\;\; f_p(-1,e') \to -1 + \Delta f(-1+1) = -1$$
$$x = 1+\Delta x:\;\; f_p(1+\Delta x, e') = \frac{k_1 x|x|}{(log(y))^2}, \;\; x = -1-\Delta x:\;\; f_p(-1-\Delta x, e') = -\frac{k_1 x|x|}{(log(y))^2} \tag{2.1.12}$$

The modified flow function $f_p(x,e)$, (2.1.11), is shown in Fig. 3.3 for Δx=0.2.

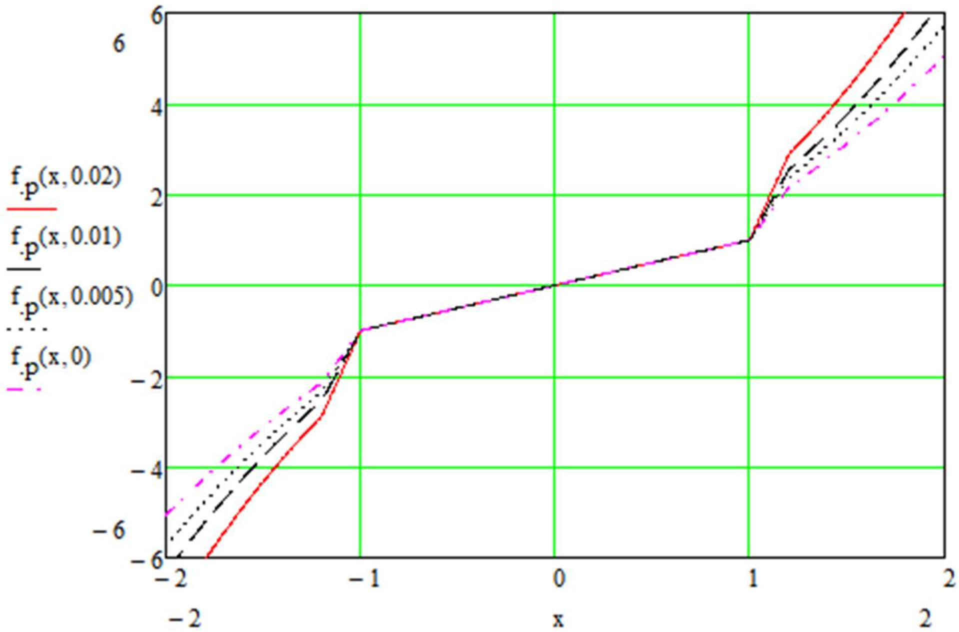

Figure 3.3. The continuous modified flow function $f_p(x,e)$.

It is again an odd function in x that increases monotonously with x. The curves show the continuous function. It follows x in -1 < x < 1. Outside the laminar region for $x > 1+\Delta x$ and $x < -1-\Delta x$, the curves differs by e'. The slope of the function is Δf in the two intermediate transition regions $1 < x < 1+\Delta x$ and $-1-\Delta x < x < -1$.

The final formula for the pressure-flow relation from (2.1.11), (2.1.6), (2.1.10) and (2.1.12) is now:

$$\Delta p = k_0 \cdot \frac{L}{D^3} \cdot f_p\left(\frac{\dot{m}}{k_2 \cdot D}, e'\right), \qquad e' = \frac{e_m}{D}. \tag{2.1.13}$$

Here, three constants are used:

$$k_0 = \frac{32\,\mu^2}{\rho} \cdot \mathrm{Re}_{\mathrm{tr}}, \qquad k_1 = \frac{\mathrm{Re}_{\mathrm{tr}}}{256}. \qquad k_2 = \frac{\pi\,\mu\,\mathrm{Re}_{\mathrm{tr}}}{4}. \tag{2.1.14}$$

Flow-pressure equations for a simple network

Figure 4.1 shows a simple network connected to an accumulator tank. Figure 4.2 shows a branched simple network connected to an accumulator tank, with an interconnection AB between the two main pipe couples A and B.

In the simple network, Figure 4.1, there are 3 supply lines (a) connected to a main pipe (A). In the branched and interconnected network there are 3+3 supply lines (six customers) connected to A and B respectively. The pipes A and B are interconnected by the pipe couple AB. The upper indices a and b refers to the supply pipes connected to the main pipes, referred to as A and B.

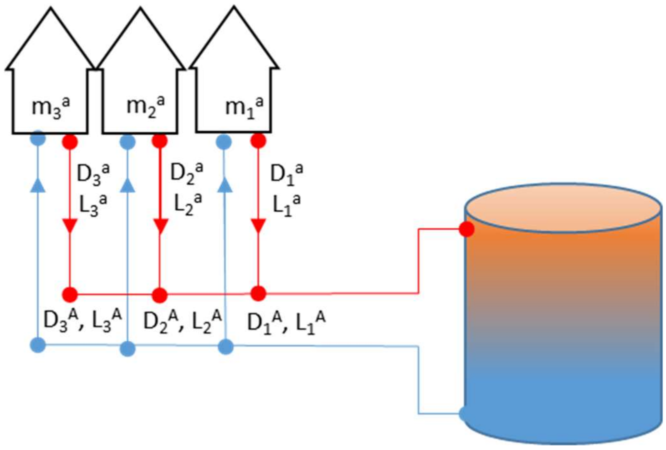

Figure 4.1. Simple network with accumulator tank, a main pipe line (A) and 3 supply lines (a) with prescribed mass flows. Red: hot or tepid side. Blue: cold side.

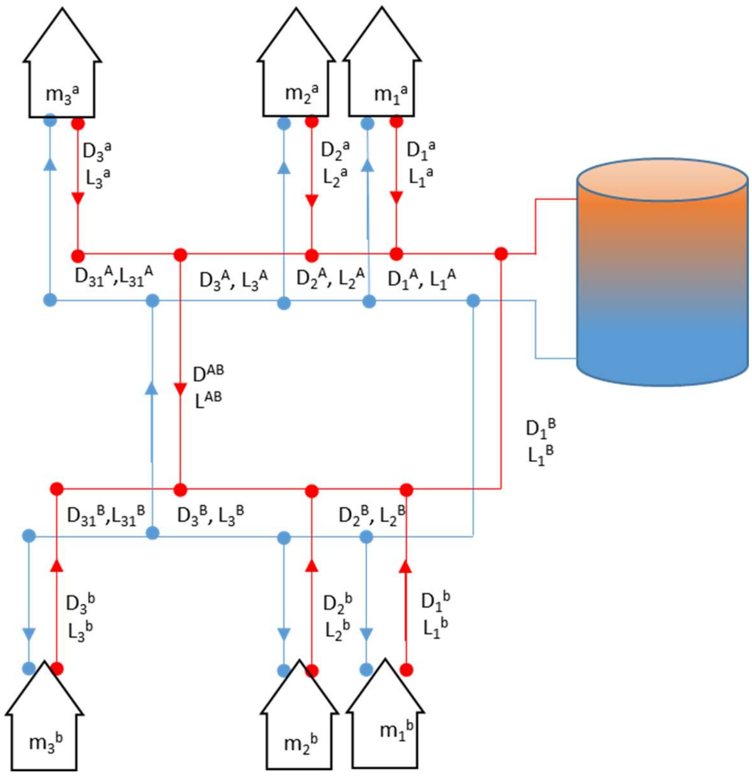

Figure 4.2. Branched simple network with accumulator tank, two main pipe lines A and B, and 3+3 supply lines with prescribed mass flows and an interconnection AB. Red: hot or tepid side. Blue: cold side.

All pipe couples have a warm or tepid pipe shown in red, and a cold pipe shown in blue. The cooling or heating demand from each customer determines the required mass flows $\dot{m}_i^a$ and $\dot{m}_i^b$, *i* = 1, 2, 3. The mass flow depends upon: the thermal power demand, *P* (kW) of the customer; the temperature difference, d_t (k), between the warm and the cold side: and the heat capacity of the medium, c_p (kJ/kgK).

$$\dot{m}_i = \frac{P}{cp * dt} \tag{3.1.1}$$

These mass flows may be positive or negative (or zero). For positive $\dot{m}_1^a$, the flow is downward in the red pipe and upward in the blue pipe following the arrows in Figure 4.1. For negative $\dot{m}_1^a$, the flows are reversed, with upward flow in the red pipe and downward in the blue pipe.

Five values for the diameters of pipe segments will be used: D_A, D_B, D_{AB}, D_a and D_b. The length of each pipe segments is an input. As shown in Fig. 2.2, the input of pipe diameters and length of pipe segments are:

$$D_i^A,\ D_i^B,\ D_{AB},\ D_i^a,\ D_i^b;\quad L_i^A,\ L_i^B,\ L_i^a,\ L_i^b,\quad i=1,2,3;\qquad L_{AB},\ L_{31}^A,\ L_{31}^B,\ D_{31}^A,\ D_{31}^B; \tag{3.1.2}$$

The flows in the pipes and the pressures in the nodes between pipes are determined by the prescribed mass flows from the 6 customers.

$$\dot{m}_i^a,\quad \dot{m}_i^b,\quad i=1,2,3. \tag{3.1.3}$$

All these flows are positive, zero or negative.

Equation for the simple network

In figure 4.3 the notations for mass flow and node pressures are given. These pressure values are above the static pressure in the grid. The static pressure occurs at the accumulator and the dynamic pressure at the accumulator is set to zero.

The warm (red) pipes are shown while the parallel (blue) pipes are omitted. The flow in any cold blue pipe has the same magnitude as that of the parallel warm red pipe but it flows in the opposite direction. The excess pressures in the cold nodes have the same magnitude as the red ones but opposite signs. As the warm and cold quantities only differ by sign, it is sufficient to only present graphically one side, in this case the warm side.

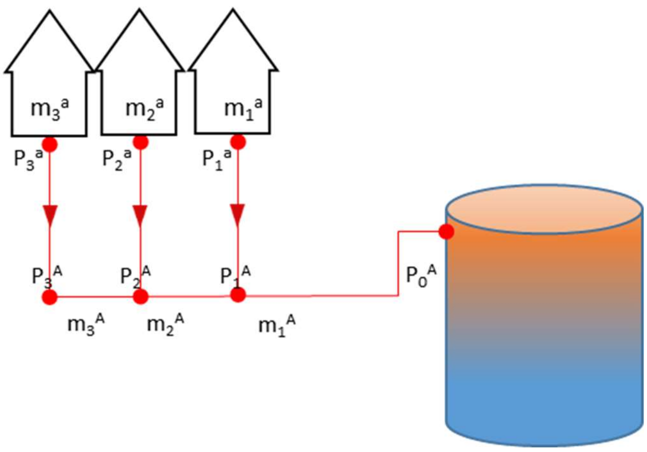

Figure 4.3. Notation for mass flows and node pressures.

The node pressures are calculated in the following way. The pressure-flow relation (2.1.13), is applied to the three right-hand segments of pipe A. The mass flows for each segment are shown in Fig. 2.3. The three input flows for pipe A become:

$$\dot{m}_3^A = \dot{m}_3^a, \qquad \dot{m}_2^A = \dot{m}_2^a + \dot{m}_3^a, \qquad \dot{m}_1^A = \dot{m}_1^a + \dot{m}_2^a + \dot{m}_3^a. \tag{3.1.4}$$

This gives accumulated input sums for pipe A:

$$\dot{m}_i^A = \sum_{j=i}^{3} \dot{m}_j^a, \qquad i = 1, 2, 3. \tag{3.1.5}$$

Formula (2.1.13) becomes for the three segments (P_{1A}- P_{3A})of pipe A:

$$p_i^A - p_{i-1}^A = k_0 \cdot \frac{L_i^A}{(D_i^A)^3} \cdot f_p\left(\frac{\dot{m}_i^A}{k_2 D_i^A}, \frac{e_m}{D_i^A}\right), \quad i = 1, 2, 3; \qquad p_0^A = 0. \tag{3.1.6}$$

And by this, each pressure node in the main supply line can be calculated.

For calculating the pressure in the whole network, we also need to calculate the pressure levels of the inlet nodes a (P_{1a}-P_{3a}):

$$p_i^a - p_i^A = k_0 \cdot \frac{L_i^a}{(D_i^a)^3} \cdot f_p\left(\frac{\dot{m}_i^a}{k_2 D_i^a}, \frac{e_m}{D_i^a}\right), \qquad i = 1, 2, 3. \tag{3.1.7}$$

Now the pressure levels and the mass flows are known for the simplest grid.

Equation for the bifurcation flow

Figure 4.4 shows the notations for the mass flows in each pipe section and the pressures at each node in the inner loop defined by pipe A, B and AB. The pressures here are the value above the static pressure in the grid. The dynamic pressure at the accumulator is set to zero.

The cross flow $\dot{m}_{AB}$ from pipe A to pipe B is unknown so has to be calculated. The flow $\dot{m}_3^A$ from the left at the node with the pressure P_3^A is divided into the downward flow $\dot{m}_{AB}$ and a remaining part $\dot{m}_3^A - \dot{m}_{AB}$ flowing to the right in pipe A. This is a kind of "*bifurcation"* flow. When opposite signs appear, the flow travels in the opposite direction compared to the arrow.

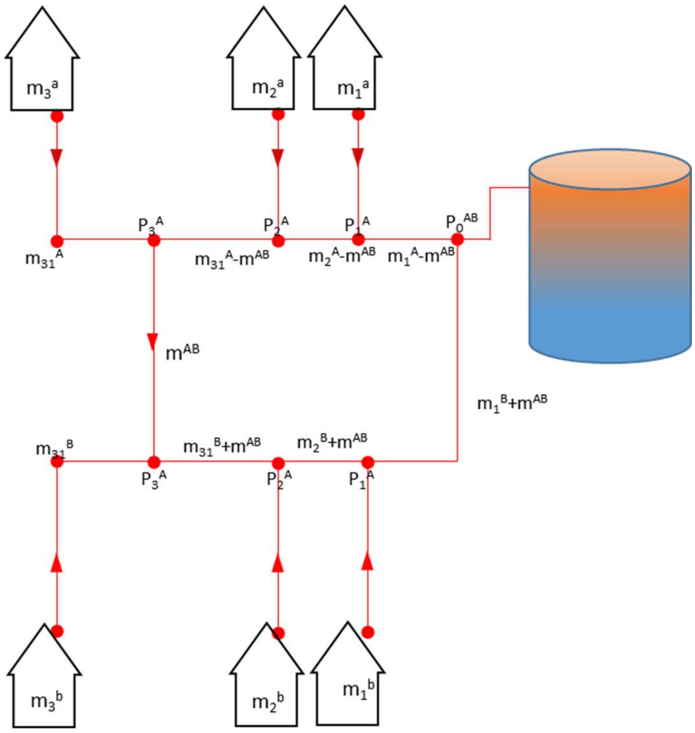

Figure 4.4. Notation for mass flows and pressure nodes of the main pipes.

The bifurcation flow is determined in the following way. The pressure-flow relation (2.1.13), is applied to the three right-hand segments of pipe A and pipe B. The mass flows for each one of the six segments are shown in Fig. 4.2 Here, the flows contain the bifurcation flow with opposite signs for A and B. The remaining part is determined by the prescribed input flows from the customers. The three input flows for pipe A become:

$$\dot{m}_3^A = \dot{m}_3^a, \qquad \dot{m}_2^A = \dot{m}_2^a + \dot{m}_3^a, \qquad \dot{m}_1^A = \dot{m}_1^a + \dot{m}_2^a + \dot{m}_3^a. \tag{3.1.8}$$

This gives accumulated input sums for pipe A and corresponding sums for pipe B:

$$\dot{m}_i^A = \sum_{j=i}^{3} \dot{m}_j^a, \qquad \dot{m}_i^B = \sum_{j=i}^{3} \dot{m}_j^b, \quad i = 1, 2, 3. \tag{3.1.9}$$

Formula (2.1.13) becomes for the three right-hand segments of pipe A (P_{1A} to P_{3A}):

$$p_i^A - p_{i-1}^A = k_0 \cdot \frac{L_i^A}{(D_i^A)^3} \cdot f_p\left(\frac{\dot{m}_i^A - \dot{m}_{AB}}{k_2 D_i^A}, \frac{e_m}{D_i^A}\right), \quad i = 1, 2, 3; \qquad p_0^A = 0. \tag{3.1.10}$$

The dynamic pressure over the accumulator is set to zero. The same type of expression is valid for pipe B (P_{1B} to P_{3B}).

$$p_i^B - p_{i-1}^B = k_0 \cdot \frac{L_i^B}{(D_i^B)^3} \cdot f_p\left(\frac{\dot{m}_i^B + \dot{m}_{AB}}{k_2 D_i^B}, \frac{e_m}{D_i^B}\right), \quad i = 1, 2, 3; \qquad p_0^B = 0. \tag{3.1.11}$$

The sum of the equations for pipe A minus the sum for pipe B becomes equal to the pressure over pipe segment AB:

$$\sum_{i=1}^{3}\left(p_i^A - p_{i-1}^A\right) - \sum_{i=1}^{3}\left(p_i^B - p_{i-1}^B\right) = p_3^A - p_0^A - \left(p_3^B - p_0^B\right) = p_3^A - p_3^B. \qquad (3.1.12)$$

The pressure over segment AB is:

$$p_3^A - p_3^B = k_0 \cdot \frac{L_{AB}}{(D_{AB})^3} \cdot f_p\left(\frac{\dot{m}_{AB}}{k_2 D_{AB}}, \frac{e_m}{D_{AB}}\right). \qquad (3.1.13)$$

The following equation is obtained from (3.1.12), (3.1.10), (3.1.11) and (3.1.13):

$$\sum_{i=1}^{3}\frac{L_i^A}{(D_i^A)^3} \cdot f_p\left(\frac{\dot{m}_i^A - \dot{m}_{AB}}{k_2 D_i^A}, \frac{e_m}{D_i^A}\right) - \sum_{i=1}^{3}\frac{L_i^B}{(D_i^B)^3} \cdot f_p\left(\frac{\dot{m}_i^B + \dot{m}_{AB}}{k_2 D_i^B}, \frac{e_m}{D_i^B}\right) = \frac{L_{AB}}{(D_{AB})^3} \cdot f_p\left(\frac{\dot{m}_{AB}}{k_2 D_{AB}}, \frac{e_m}{D_{AB}}\right).. \qquad (3.1.14)$$

This gives the following basic equation to determine the bifurcation flow $\dot{m}_{AB}$:

$$\boxed{\frac{L_{AB}}{(D_{AB})^3} \cdot f_p\left(\frac{\dot{m}_{AB}}{k_2 D_{AB}}, \frac{e_m}{D_{AB}}\right) + \sum_{i=1}^{3}\frac{L_i^A}{(D_i^A)^3} \cdot f_p\left(\frac{-\dot{m}_i^A + \dot{m}_{AB}}{k_2 D_i^A}, \frac{e_m}{D_i^A}\right) + \sum_{i=1}^{3}\frac{L_i^B}{(D_i^B)^3} \cdot f_p\left(\frac{\dot{m}_i^B + \dot{m}_{AB}}{k_2 D_i^B}, \frac{e_m}{D_i^B}\right) = 0.} \qquad (3.1.15)$$

Here, the fact that $f_p(x,e')$ is an odd function of x is used. The sum in the middle is the same as the left-hand sum in (3.1.14), but with a changed sign for the mass flow.

The left-hand function in (3.1.15), may be represented in the following way:

$$x = \frac{\dot{m}_{AB}}{k_2 D_{AB}}, \frac{e_m}{D_{AB}}: \quad f_{\mathrm{pb}}(x,e') = \frac{L_{AB}}{(D_{AB})^3} \cdot f_p(x) + \sum_{i=1}^{3}\frac{L_i^A}{(D_i^A)^3} \cdot f_p\left(\frac{-\dot{m}_i^A}{k_2 D_i^A}, \frac{e_m}{D_i^A} + \frac{D_{AB}}{D_i^A} \cdot x\right) + \\ + \sum_{i=1}^{3}\frac{L_i^B}{(D_B)^3} \cdot f_p\left(\frac{\dot{m}_i^B}{k_2 D_i^B}, \frac{e_m}{D_i^B} + \frac{D_{AB}}{D_i^B} \cdot x\right). \qquad (3.1.16)$$

The solution for the bifurcation flow (m_{ab}) is given by the root of $f_{\mathrm{pb}}(x)$ = 0:

$$f_{\mathrm{pb}}(x_{AB}, e') = 0, \qquad \dot{m}_{AB} = k_2 D_{AB} \cdot x_{AB}. \qquad (3.1.17)$$

It should be noted that all seven terms in (3.1.16) are, just as $f_p(x)$, monotonously increasing and continuous functions of x. The root or zero value can be simply determined, and the solution should be quite robust.

Pressure-flow relations for the whole network

Figure 4.5 shows the mass flows for all pipe segments and the accumulator. The inlet mass flows (3.1.3) are prescribed. The other mass flows are given by (3.1.9) and (3.1.17). The remaining task is now to determine all node pressures.

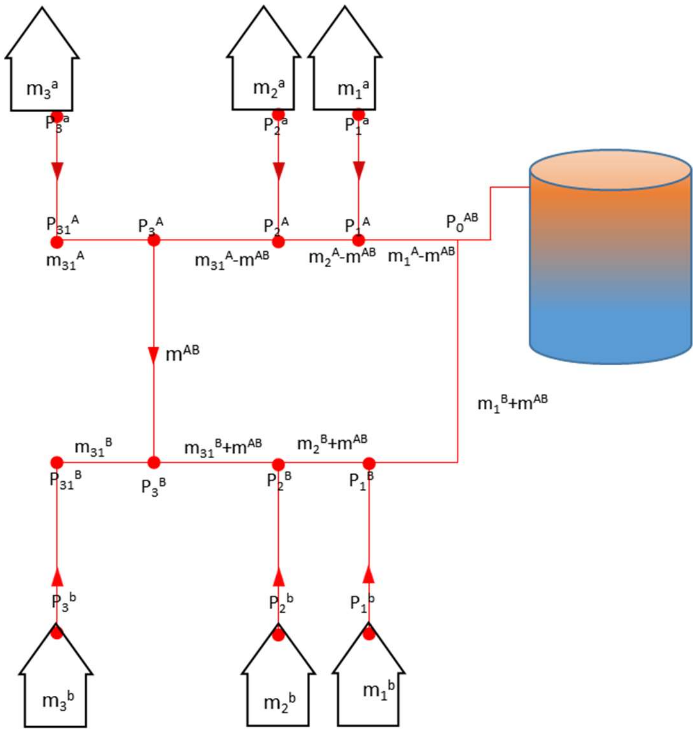

Figure 4.5. Mass flows for all pipe segments and water pressures at all pressure nodes.

The three right-hand node pressures along pipe A, up the bifurcation node, are given by (3.1.10) and the corresponding pressures along pipe B by (3.1.11). The pressures at node "P_{31}" on pipe A and B are given by:

$$p_{31}^A - p_3^A = k_0 \cdot \frac{L_{31}^A}{(D_{31}^A)^3} \cdot f_p\left(\frac{\dot{m}_{31}^A}{k_2 D_{31}^A}, \frac{e_m}{D_{31}^A}\right), \qquad p_{31}^B - p_3^B = k_0 \cdot \frac{L_{31}^B}{(D_{31}^B)^3} \cdot f_p\left(\frac{\dot{m}_{31}^B}{k_2 D_{31}^B}, \frac{e_m}{D_{31}^B}\right). \qquad (3.1.18)$$

The pressure at the two right-hand inlet nodes (P_{1a} and P_{2aa}) on the A and B side become:

$$p_i^a - p_i^A = k_0 \cdot \frac{L_i^a}{(D_i^a)^3} \cdot f_p\left(\frac{\dot{m}_i^a}{k_2 D_i^a}, \frac{e_m}{D_i^a}\right), \qquad p_i^b - p_i^B = k_0 \cdot \frac{L_i^b}{(D_i^b)^3} \cdot f_p\left(\frac{\dot{m}_i^b}{k_2 D_i^b}, \frac{e_m}{D_i^b}\right), \qquad i = 1, 2. \qquad (3.1.19)$$

Finally, the pressures at the leftmost inlet nodes (P_{3a} and P_{3b}) become:

$$p_3^a - p_{31}^A = k_0 \cdot \frac{L_3^a}{(D_3^a)^3} \cdot f_p\left(\frac{\dot{m}_3^a}{k_2 D_3^a}, \frac{e_m}{D_3^a}\right), \qquad p_3^b - p_{31}^B = k_0 \cdot \frac{L_3^B}{(D_3^b)^3} \cdot f_p\left(\frac{\dot{m}_3^b}{k_2 D_3^b}, \frac{e_m}{D_3^b}\right). \qquad (3.1.20)$$

An example of flow and pressure calculation of a 5GDHC two pipe solution

In this part, a pressure and flow calculation of a shared energy system, (SES grid) with six interconnected buildings with various power demands is performed. The grid is designed as in Figure 5.1 and the input data used is related to the indexation in the same Figure.

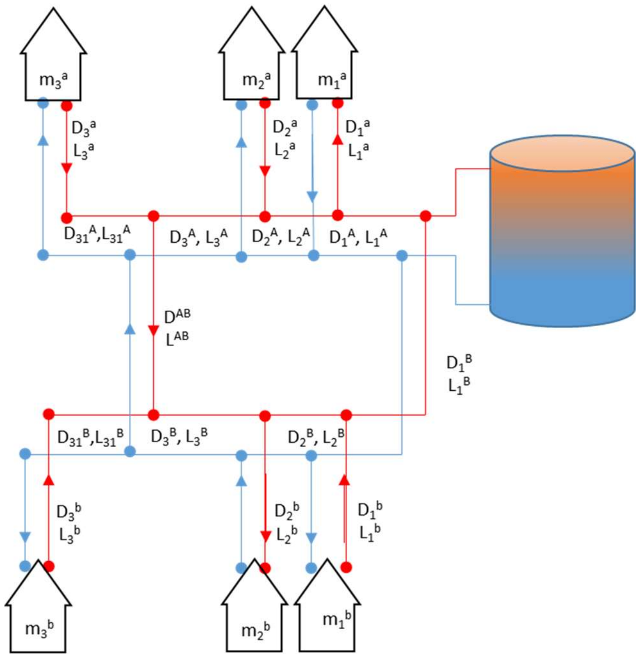

Figure 5.1: Grid design

The following input data will be used:

$$\rho = 999{,}1\ (\mathrm{kg/\,m^3}), \qquad \mu = 1\cdot 10^{-3}\ (\mathrm{kg/(m,s)}), \qquad \mathrm{Re}_{\mathrm{tr}} = 2\,000, \qquad \Delta x = 0.2. \tag{4.1.1}$$

The three constants (2.1.14) become:

$$k_0 = 6{,}4\cdot 10^{-5}, \qquad k_1 = 7{,}8125. \qquad k_2 = 1{,}571 \tag{4.1.2}$$

Table 5.1: Input data for pressure flow calculations

Indata for flow and pressure calculation											
Position	Massflow (kg/s)	Position	Diameter (mm)	Inner diameter (mm)	Position	Length (m)	Position	Diameter (mm)	Inner diameter (mm)	Position	Length (m)
m_1^a	-4,8	D_1^a	75	66	L_1^a	5	D_1^A	160	141	L_1^A	17,8
m_2^a	15,6	D_2^a	110	96,8	L_2^a	73,6	D_2^A	140	123,4	L_2^A	122,9
m_3^a	7,2	D_3^a	75	66	L_3^a	18	D_3^A	75	66	L_3^A	46,3
m_1^b	14,4	D_1^b	75	66	L_1^b	73,8	D_1^B	110	96,8	L_1^A	70,1
m_2^b	-9,6	D_2^b	110	96,8	L_2^b	46,1	D_2^B	110	96,8	L_2^B	37,1
m_3^b	6,0	D_3^b	110	96,8	L_3^b	123,9	D_3^B	75	66	L_3^B	44,4
							D_{31}^A	75	66	L_{31A}	10
							D_{31}^B	75	66	L_{31}^B	120
							D^{AB}	75	66	L^{AB}	128,2

The first step is to calculate the pressure difference between A & B, (that results in the cross flow). Note that the differential pressure over the accumulator is set to 0.

To determine the cross flow we start by calculating the mass flow of pipe A and pipe B. Applying equation (3.1.9) determines the massflow of each side without any bifurcation, see Figure 4.4.

Table 5:2 Mass flow in the inner loop without bifurcation.

massflow without bifurcation	
Position	Massflow (kg/s)
m_1^A	18
m_2^A	22,8
m_3^A	7,2
m_1^B	10,8
m_2^B	-3,6
m_3^B	6

Using the mass flows of each node in (3.1.16) and (3.1.17) the mAB is calculated.

mAB= 1,3 kg/s

The flow relation in the whole network is described in Figure 4.5. The calculated mass flows are shown in table 5.3.

Table 5.3: Mass flows in the whole grid with bifurcation

massflow bifurcation	
Position	Massflow (kg/s)
$m_1^A - m^{AB}$	16,7
$m_2^A - m^{AB}$	21,5
$m_3^A - m^{AB}$	5,9
m_{31}^A	7,2
$m_1^B+m^{AB}$	12,1
$m_2^B+m^{AB}$	-2,3
$m_3^B+m^{AB}$	7,3
m_{31}^B	6
m^{AB}	1,3

The pressure nodes in the grid can now be calculated with equations (3.1.10), (3.1.11), (3.1.18), (3.1.19) and (3.1.20) the positions is related to Figure 2.5. These are shown in table 5.4.

Table 5.4: Pressure in the whole grid

Pressure in the whole grid			
Position	Pressure (Pa)	Position	Pressure (Pa)
p_1^A	1228	p_1^a	-187
p_2^A	26995	p_2^a	54917
p_3^A	46304	p_3^a	57012
p_{31}^A	52253		
p_1^B	16577	p_1^b	175618
p_2^B	16123	p_2^b	8949
p_3^B	42984	p_3^b	51196
p_{31}^B	94057		
p^{AB}	3320		

Now all flow and pressure levels are known in the grid.

Local losses

The influence on pressure related to local losses from fittings, such as bends, valves and T-pipes, in a district grid is normally low due to the size of the pipes and the frequency of fittings. But even if the influence of the fittings is modest, it is possible to include local pressure losses to the calculation and make the calculation even more precise.

A common way of handling the influence of the fittings is by using the equivalent length method. The method is easy to use and calculate, but its weakness is that the method is no stronger than the accuracy of the loss coefficient ζ. Typical values of ζ can be retrieved from manufacturers or in different handbooks such as Handbook of hydraulic resistance or the Heat Atlas [15][16] The theory is to define the characteristic / pressure drop that a certain fitting causes as a corresponding pipe length. By using this method, it is possible to calculate the total pressure demand by just adding additional pipe length that compensates for the fittings.

By setting formula (3.1.3) equal to the formula of local pressure losses, Δp_{local}

$$\Delta p_{local} = \zeta * \frac{\rho u^2}{2}, \tag{5.1.1}$$

where ζ is a tabulated value for the specific fitting.

The equivalent length can be calculated as:

$$L_{eq} = D \cdot \frac{\zeta}{cf} = D \cdot \zeta \cdot 4(\log(y))^2. \tag{5.1.2}$$

If the influence of pipe roughness is considered negligible, the L_{eq} can be calculated as:

$$L_{eq} = D \cdot \frac{\zeta}{cf} = D \cdot \frac{\zeta}{0,316} \cdot \mathrm{Re}^{0,25} \ .$$

Discussion:

The aim of this work is to design a continuous formula to be used for pressure and mass flow calculations in 5GDHC solutions with a meshed grid and non-directional medium flow. The Swamee-Jain formula was chosen for calculating the friction factor since it takes pipe roughness into account. The possibility of calculating pressure levels and mass flows of a 5GDHC grid is valuable in many ways. That knowledge can be used for optimising the operation and design. It can also be used to predict what to expect from such a grid.

Knowing how the flows divide within the grid makes it possible to calculate energy leakage from the grid or the energy recovery from surrounding soil. Calculating pressure levels in the grid enables prediction of energy costs for pumping and can also be a tool for designing operation strategies and equipment. The calculation can also be applied as a monitoring tool, to identify deviations and indicate disturbances.

In the design phase, this knowledge highlights the consequences when choosing pipe diameters and also provides essential design parameters for local circulation pumps.

The calculation also gives vital information when expanding a grid. For example, by calculating the new pressure, measures to avoid exceeding the pressure limits of the grid can be implemented, such as increasing the temperature difference or meshing the grid. If the calculation method is used for this purpose, the static pressure must also be added to the equation.

During the design phase, local losses in a grid are either overlooked or a simple percentage compensation is used. A better but more demanding method to include the local losses in the calculation is the equivalent length method.

When calculating pressure losses in a pipe system with turbulent flow, the pipe roughness influences the pressure loss. In the presented grid calculation method, the roughness is taken into account. Some 5GDHC will be designed with plastic pipes material and if so the pipes can be assume to be smooth and with a small influence of pipe roughness. We have estimated the error to be low based upon the following reasoning.

- The diameter of the pipes in a grid with a low DT is large, often >100 mm.
- The Reynolds number is normally beyond 1*10^6 in such systems.
- The piping material is mainly based upon plastic pipes with low absolute roughness

The absolute roughness of district heating pipes is around 0,05 and for plastic pipes it is 0,01 mm (stated by manufacturers and industrial organization such as Powerpipe and Nordic plastic pipe association)[17][18]. For a 100 mm diameter pipe, this results in a low relative roughness (<0,0005-0,0001) and, as a consequence, a low difference in friction factor between smooth pipes and plastic pipes up to RE 1*10^5.

It is also worth remembering that the point of dimensioning the system is based on the “worse” case which differs a lot from the ordinary operation point with a much lower Reynolds number. This limits the error of the friction factor even more when used for calculation over a period of time, such as calculating energy demand.

A formula calculating the pressure drop without taking pipe roughness into account, based upon Blasius formula for calculating c_f will look like:

$$\Delta p = k_0 \cdot \frac{L}{D^3} \cdot f_p\left(\frac{\dot{m}}{k_2 \cdot D}\right), \qquad f_p(x) = \begin{cases} x & \left|x\right| < 1 \\ k_1\, x\, \left|x\right|^{0.75} & \left|x\right| > 1 + \Delta x \\ 1 + k_3(x-1) & 1 < x < 1 + \Delta x \\ -1 + k_3(x+1) & -1 - \Delta x < x < -1 \end{cases} \tag{6.1.1}$$

Here, four constants are used:

$$k_0 = \frac{32\,\mu^2}{\rho} \cdot \mathrm{Re}_{\mathrm{tr}}, \quad k_1 = \frac{0.079}{16} \cdot \mathrm{Re}_{\mathrm{tr}}^{0.75}, \quad k_2 = \frac{\pi\,\mu\,\mathrm{Re}_{\mathrm{tr}}}{4}, \quad k_3 = \frac{k_1 \cdot (1 + \Delta x)^{1.75} - 1}{\Delta x}. \tag{6.1.2}$$

If using Blasius formula instead, it is important to be aware of the limitation despite the calculation working reliably under “ordinary” circumstances with plastic pipe qualities.

Calculation methods using reference point as a base together with the affinity laws that states that the dynamic pressure is proportional to the square of flow to calculate different loads, starts with a traditional pressure loss calculation such as Darcy-Weisbach and the moody diagram to retrieve the design/reference point as a base to calculate from. This method requires retrieving the friction factor from the Moody-Brooke diagram and then calculating the pressure drop of the reference point, using the Darcy- Weisbach method. From there, based on the square relation between flow and pressure changes, a new pressure level can be calculated.

The slightest changes of the grid design require a whole new calculation of the design/reference point. The square relation between flow and pressure is also not exactly square, so a small deviation appears, and how big it is depends upon how big the changes are from the reference point and the square relation is only valid within the turbulent area.

With the presented continuous formula it is possible to calculate the pressures and flows in the grid when loads or the design changes. This is much easier and accurate to use in dynamic simulation programs or for evaluating different design solutions.

A comparison between calculation methods (1.1.1) and (2.1.13) is conducted, assuming that the results from pressure calculations using Darcy-Weisbach formula combined with retrieving the friction factor (cf) from the moody diagram gives the true pressure.

The comparison is performed by a number of pressure loss calculations of a pipe with a length of 100 m and a diameter of 0,1 m and with different Reynolds numbers. The choice of Reynolds numbers is performed to cover the width of the moody diagram but also more frequently in the more common part of the moody diagram. Looking at the equation 1.3 it shows that a change of Reynolds number in a pipe with the same medium and temperature can only be achieved by changing the velocity and by that the mass flow.

In the method using the affinity law, the first step is a pressure loss calculation, using, for example, the Darcy-Weisbach method, to retrieve design/reference point to go from. The next step is to calculate, based on the base point, the new pressure loss a changed medium flow causes. This is performed by using the square relation between flow and pressure. In our comparison, the design/reference point is chosen to be where the Reynolds number is 1 * 10 ^ 5.

The following assumptions have been used:

e ’= 0.0002, D = 0.1m, Viscosity = 0.001kg / m·s, ρ = 999.1kg / m3, Retr = 2300, and L = 100m K = 1.

Based on those assumptions the three different methods are used and the results are presented in the table below:

Table 7.1: Comparison between calculation methods

Results:								
Re	u (m/s)	*cf*	Δp_{darcy} (Pa)	Δp_{aff} (Pa)		Deviation	Δp_{cont} (Pa)	Deviation
1000	0,010009	0,064	3		1	0,30	3	1,00
10000	0,10009	0,031	155		95	0,61	157	1,01
50000	0,50045	0,0215	2690		2377	0,88	2696	1,00
100000	1,000901	0,019	9509	Design point	9509		9506	1,00
200000	2,001802	0,017	34031		38034	1,12	34294	1,01
300000	3,002702	0,0162	72966		85577	1,17	73460	1,01
400000	4,003603	0,0157	125713		152137	1,21	126758	1,01
500000	5,004504	0,0154	192673		237714	1,23	194070	1,01
600000	6,005405	0,0151	272045		342308	1,26	275331	1,01
700000	7,006306	0,015	367831		465919	1,27	370500	1,01
800000	8,007206	0,01485	475628		608548	1,28	479546	1,01
900000	9,008107	0,0148	599940		770193	1,28	602452	1,00
1000000	10,00901	0,0147	735662		950856	1,29	739202	1,00
10000000	100,0901	0,0136	68061255		95085577	1,40	69441110	1,02

As shown in the table, the deviations between the continuous method and the Darcy-Weisbach method is very low. The method based on the affinity laws differs more and especially within the laminar area, where the formula is not applicable.

Even though the deviations are larger when using the affinity laws, it might be sufficiently accurate enough within a normal operating area. Where the velocity in the pipe goes between the initial turbulence velocity and 3 m/s, then the deviation in our comparison goes up to 17%.

By using the continuous calculation method it is possible to:

- Both retrieve the pressure drop and the mass flows directly in a meshed grid with non-directional medium flow and bidirectional energy flow
- The calculation method handles changes of the grid configuration directly which makes it more suitable for pre-design and simulation purposes.
- The deviations is low compared to Darcy-Weisbach which is a well-established method, and hopefully the method can be implemented as a tool for monitoring the operation of the grid so identify unexpected local pressure losses.

There are needs for further tests and verification of the method and it would be valuable to test the method on a real facility.

Conclusion:

With this calculation method, it is possible to determine the pressure and mass flow in each part of the grid and it is possible to calculate each point directly without the reference point. The consequences if changing the conditions such as pipe radius or length is also handled by the calculation method. The proposed calculation method can be used both as a design and a simulation tool.

The calculation method handles a meshed grid bifurcation flows and if the grid has lots of fittings that gives local pressure losses it can be handled using the equivalent length (Leq) method. There are demands for further investigation on how to handle multiple loops within the grid.

The outcome can be used for identifying bottlenecks when expanding a grid or used as a dimensioning tool, to determine the pipe dimensions in the grid and/or the pressure demands and calculate design parameters for local circulation pumps. It can be used to determine the consequences of expanding the grid or increasing local power demands and be a tool for decision making.

Knowing how the water moves (mass flows) in the grid makes it possible to calculate energy losses or gains in the grid.

This report is a part of the work in developing a calculation tool for grids with bidirectional energy and non-directional medium flows. This calculation method will be a part of a modelica based simulation tool for 5GDHC systems that is under development.

References:

[1] European Commission, "An EU Strategy on Heating and Cooling," *J. Chem. Inf. Model.*, vol. 53, no. 9, pp. 1689–1699, 2016.

[2] M. Pellegrini and A. Bianchini, "The innovative concept of cold district heating networks: A literature review," *Energies*, vol. 11, no. 2, 2018.

[3] N. Long, "Reduced Order Models for Rapid Analysis of Ambient Loops for Commercial Buildings," p. 208, 2018.

[4] H. Lund *et al.*, "4th Generation District Heating (4GDH). Integrating smart thermal grids into future sustainable energy systems.," *Energy*, vol. 68, pp. 1–11, 2014.

[5] T. Sommer, M. Sulzer, M. Wetter, A. Sotnikov, S. Mennel, and C. Stettler, "The reservoir network: A new network topology for district heating and cooling," *Energy*, vol. 199, 2020.

[6] F. Bünning, M. Wetter, M. Fuchs, and D. Müller, "Bidirectional low temperature district energy systems with agent-based control: Performance comparison and operation optimization," *Appl. Energy*, vol. 209, no. November 2017, pp. 502–515, 2018.

[7] M. Wetter, "Modelica Buildings Library Michael Wetter , Wangda Zuoa , Thierry S .," 2015.

[8] M. Wetter, "Modelica Library for Building Heating, Ventilation and Air-Conditioning Systems," *Proc. 7 Int. Model. Conf. Como, Italy*, vol. 43, pp. 393–402, 2009.

[9] B. van der Heijde *et al.*, "Dynamic equation-based thermo-hydraulic pipe model for district heating and cooling systems," *Energy Convers. Manag.*, vol. 151, no. September, pp. 158–169, 2017.

[10] N. G. Christoph *et al.*, "Iea ebc annex 60 modelica library - An international collaboration to develop a free open-source model library for buildings and community energy systems," *14th Int. Conf. IBPSA - Build. Simul. 2015, BS 2015, Conf. Proc.*, no. April 2016, pp. 395–402, 2015.

[11] "A technical design framework for cold heating and cooling."

[12] Vitec, "Användarmanual NetSim," 2013.

[13] "Modelica standard library." [Online]. Available: https://doc.modelica.org/Modelica 4.0.0/Resources/helpDymola/Modelica_Fluid_Pipes_BaseClasses_WallFriction.html#Modelica .Fluid.Pipes.BaseClasses.WallFriction.

[14] J. A. Shercliff, " An Introduction to Fluid Mechanics and Heat Transfer , by J. M. K AY . Cambridge University Press, 1957. 309 pp. 37 s . 6 d . or $7.00. ," *J. Fluid Mech.*, 1958.

[15] I. E. Idelchik, "Handbook of Hydraulic Resistance, 2nd Edition," *J. Press. Vessel Technol.*, vol. 109, no. 2, pp. 260–261, 1987.

[16] K. G. Schmidt, *M1 Heat Transfer to Finned Tubes*. 2010.

[17] Nordiska Plaströrsgruppen, "Tryckrörssystem av polyeten (pe)," p. 26, 2011.

[18] O. Series *et al.*, "Product Catalogue 2020," 2020.